Electron thermalization and trapping rates in pure and doped alkali and alkaline-earth iodide crystals studied by picosecond optical absorption

K. B. Ucer,[1,*] G. Bizarri,[2] A. Burger,[3] A. Gektin,[4] L. Trefilova,[4] and R. T. Williams[1]

[1]*Department of Physics, Wake Forest University, Winston-Salem, North Carolina 27109, USA*

[2]*Lawrence Berkeley National Laboratory, Berkeley, California 94720, USA*

[3]*Department of Life and Physical Science, Fisk University, Nashville, Tennessee 37208, USA*

[4]*Institute for Scintillation Materials NAS, 60 Lenin Avenue, Kharkov 61001, Ukraine*

(Received 11 February 2014; revised manuscript received 19 March 2014; published 10 April 2014)

Although light continues to be emitted from insulating crystals used as scintillators over a period of nanoseconds to microseconds after stopping of an energetic particle, much of what determines the nonlinearity of response goes on in the first picoseconds. On this time scale, free carriers and excitons are at high density near the track core and thus are subject to nonlinear quenching. The hot (free) electrons eventually cool to low enough energy that trapping on holes, dopants, or defects can commence. In the track environment, spatial distributions of trapped carriers determined on the picosecond time scale can influence the proportionality between light yield and the initial particle energy throughout the whole light pulse. Picosecond spectroscopy of optical absorption induced by a short pulse of above-gap excitation provides a useful window on what occurs during the crucial early evolution of excited populations. The laser excitation can be tuned to excite carriers that are initially very hot (∼3 eV) relative to the band edges, or that are almost thermalized (∼0.1 eV excess energy) at the outset. Undoped and doped samples of NaI:Tl(0%, 0.1%), CsI:Tl(0%, 0.01%, 0.04%, 0.3%), and SrI_2:Eu(0%, 0.2%, 0.5%, 3%) are studied in this work.

DOI: 10.1103/PhysRevB.89.165112 PACS number(s): 78.47.J−, 78.70.Ps, 72.20.Jv

I. INTRODUCTION

Recent experiments measuring interband photon density response found the rather startling result that nonlinear quenching of luminescence in iodide crystals including CsI and SrI_2 is nearly pure third order in excitation density when excited well above the band gap [1,2]. There is no significant contribution from second-order quenching by dipole-dipole transfer between excitons. Third order implies free-carrier Auger recombination, suggesting that in the iodide crystals of heavier metals, free carriers are the dominant excited-state population during nonlinear quenching. In NaI and CsI excited close to the band gap, mixed kinetic order of nonlinear quenching was found depending on the energy of carriers excited above the band gap in the range 0.1 to 0.4 eV. In oxides measured so far, nearly pure second-order quenching is found [1,2].

Since the alkali and alkaline-earth iodides are insulators having substantial exciton binding energy of 0.3 to 0.5 eV, there must be something preventing exciton formation during nonlinear quenching in iodides where pure third-order quenching is observed, and conversely allowing rapid formation of excitons (interacting dipole oscillators) in the oxides. It may be concluded that the physical criterion responsible for determining the dominant kinetic order of nonlinear quenching is the rate of hot electron thermalization [1,2] mediated by the optical phonon frequency ω_{LO} [1,3–6]. Li *et al.* [7] and Kerisit *et al.* [8] have shown by Monte Carlo simulations of phonon scattering that in CsI when electrons start from energies 3 to 5 eV above the conduction band minimum (cbm), excitons should not start to form in significant number until after a delay of about 3 to 4 ps, whereas in oxides such as YAP [7] or fluorides such as CaF_2 [3,4], exciton formation begins within 0.1 ps. Slow thermalization time may be the only plausible explanation of free-carrier dominance (pure third-order quenching) in iodide scintillators, and it appears to be one of the most important material parameters for prediction of scintillator proportionality and light yield [2,9,10].

Despite successes of the model of hot free carriers as the reason for dominant third-order quenching in iodide crystals, one would like to have independent experimental data on the nature of excited states existing for the first few picoseconds in these materials. Such data could shed light on fundamental processes including exciton formation, trapping, and self-trapping on the early time scale. In activated and/or codoped [11] scintillators, such measurements can provide information on trap identities and branching between fractional populations of excited states existing as free carriers, excitons, self-trapped excitons, activator-trapped charges or excitons, and charges trapped on codopants or defects. We can draw on data and analyses of previous picosecond optical absorption and other time-resolved spectroscopic studies aimed at investigating self-trapping of excitons and holes as well as lattice defect formation in alkali halides [12–16], in alkaline-earth fluorides [17,18], and in alkali iodides [19,20] specifically.

Beyond our immediate consideration of metal halide insulators and their application for scintillation radiation detectors, the methods and findings of this study overlap interests in multiphonon carrier capture and nonradiative recombination in wide-gap semiconductors for laser diode and ambient lighting applications, hot electron phenomena, and charge separation versus nonradiative recombination and deep trapping in detectors, photovoltaics, and photocatalysts. Recent progress in first-principles calculation of multiphonon capture on defects in GaN [21] establishes a framework for predicting capture rates during and after carrier thermalization that are experimentally testable by measurements such as described in this paper.

*Corresponding author: ucerkb@wfu.edu

It is the aim of this paper to survey picosecond optical absorption in accessible infrared and visible spectral ranges, induced by interband excitation of three alkali and alkaline-earth iodide materials, namely, CsI, NaI, and SrI_2. The survey includes both undoped crystals and crystals doped with the luminescence centers Tl^+ and Eu^{2+} commonly employed in the alkali halides and alkaline-earth halide, respectively, to achieve scintillation, i.e., luminescence from energy deposited initially in the crystal host. Our aim is to identify absorption signatures of as many of the excited-state species as possible, including free carriers, (self-trapped) excitons, (self-trapped) holes, and charge states of the activator ions assignable to trapped electrons, holes, or excitons. Using these signatures, it is our goal to track the excited-state populations in real time through the early part of the evolution of light that is compatible with picosecond techniques. Motivating reasons are that it is often easier to resolve picosecond and subpicosecond phenomena in optical absorption than in luminescence, and in any case the absorption viewpoint gives an alternative perspective on transport and trapping phenomena to complement luminescence data. By tuning the photon energy of the two-photon interband excitation, we can select the energy of the initial carriers and thus study the dependence of capture rate on the energy of hot electrons and their thermalization.

II. EXPERIMENT

Optical absorption induced by band-gap excitation in doped and undoped CsI, NaI, and SrI_2 samples was measured using a standard pump-probe technique with two-photon excitation of the sample as shown in Fig. 1. A portion of the output of an amplified Ti:sapphire laser running at 840 nm (1.48 eV) and 10-Hz repetition rate was used to generate either second harmonic at 420 nm (2.95 eV) or third harmonic at 280 nm (4.43 eV) to be used as the pump pulse. The samples were excited by two-photon absorption (TPA) of the pump to populate final states at 5.9 and 8.86 eV, respectively. Since NaI and CsI have room-temperature band gaps in the range of 5.8 to 5.9 eV, this allows excitation of electrons with excess kinetic energies of about 0.1 and 3 eV for second-harmonic and third-harmonic pump pulses, respectively. In this way, it is possible to observe effects of changing the initial

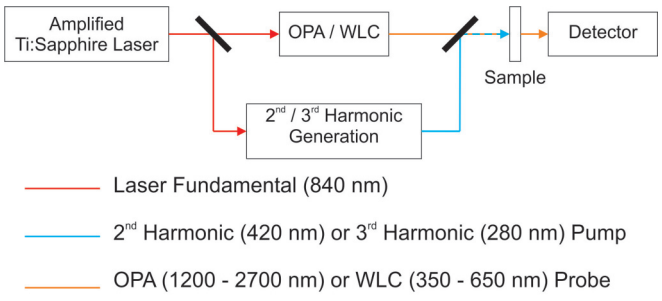

FIG. 1. (Color online) Schematic pump-probe setup for measuring transient optical absorption induced by two-photon interband absorption of the 500-fs pump pulse, probed by a delayed white light continuum pulse in the visible and near-ultraviolet spectrum or a tunable optical parametric amplifier (OPA) pulse in the infrared.

electron energy above the conduction band minimum. In SrI_2 with $E_g \sim 5.7$ eV [22,23], the initial excess energies in this experiment are slightly larger.

The energy deposited in the sample by two-photon absorption was measured by comparing transmitted to incident pump-pulse energy as a function of pulse energy. With the pump beam transverse profile measured by a CCD beam profiler (BC106-UV, Thorlabs, NJ), the two-photon absorption coefficient $\beta = 0.708$ GW/cm for CsI was deduced from fitting. For typical pump-pulse irradiance used in our absorption measurements, an excitation density of about 2.5×10^{18} eh/cm^3 was produced on the beam axis at the entrance face of the sample. Due to pump depletion, this decreased rapidly with depth into the sample, decaying to $1/e$ in about 90 μm. The measured absorption signal is thus a sum of attenuations in slabs of varying excitation density, as well as an integral over the probe pulse and excitation profile in the lateral dimension. For purposes of rough estimates of kinetic rates in the sampled volume, a typical excitation density of about half the maximum on axis at the front surface, i.e., $\sim 1.2 \times 10^{18}$ eh/cm^3, can be used in lieu of exact fitting of kinetic models. While this spatially averaged excitation density is about two orders of magnitude lower than the densities expected at the end of an electron track, it is in a similar range with average excitation densities expected in the high-energy beginning of a 662-keV electron track, probably a bit lower. Therefore, the excitation density produced in this experiment is roughly comparable to densities at which much of the energy of a high-energy gamma ray would be deposited.

For studying visible absorption, a white light continuum between 350 nm (3.54 eV) and 650 nm (1.91 eV) was used as a probe. Changes in induced transmission were recorded by an optical multichannel analyzer yielding a spectrum at each delay line setting. In the infrared, an optical parametric amplifier tunable between 1200 nm (1.03 eV) and 2700 nm (0.46 eV) probed the induced absorption as recorded by a PbS detector. In this case, we recorded a delay-line time trace at each OPA tuned wavelength. The pump and the OPA probe beam were orthogonally polarized with respect to each other. The recorded changes in induced transmission are converted to an induced change in optical density as follows:

$$\Delta(OD) = -\log_{10}\left(\frac{\Delta T}{T_0} + 1\right). \quad (1)$$

This change is with respect to any baseline of residual absorption produced under 10-Hz repetition of the pump pulses. Such residual absorption was found to be very weak in CsI and NaI, and moderate in SrI_2 at room temperature.

Samples of undoped CsI and CsI:Tl with 0.01, 0.04, and 0.3 wt % of thallium iodide in the starting material were grown by the Stockbarger technique at the Institute for Single Crystals in Kharkov, Ukraine. Samples of undoped NaI and NaI:Tl (0.1 wt % in starting material) were grown and encapsulated in cells with quartz windows at the same institute. Samples of undoped SrI_2 and SrI_2:Eu (0.2%, 0.5%, and 3% mole %) were grown and encapsulated in cells with sapphire windows at Fisk University. The segregation coefficients for Tl^+ in CsI and NaI are 0.18 and 0.20, respectively [24]. Although the figure labels and discussions refer to the nominal wt % in the starting material, it should be understood that the actual Tl

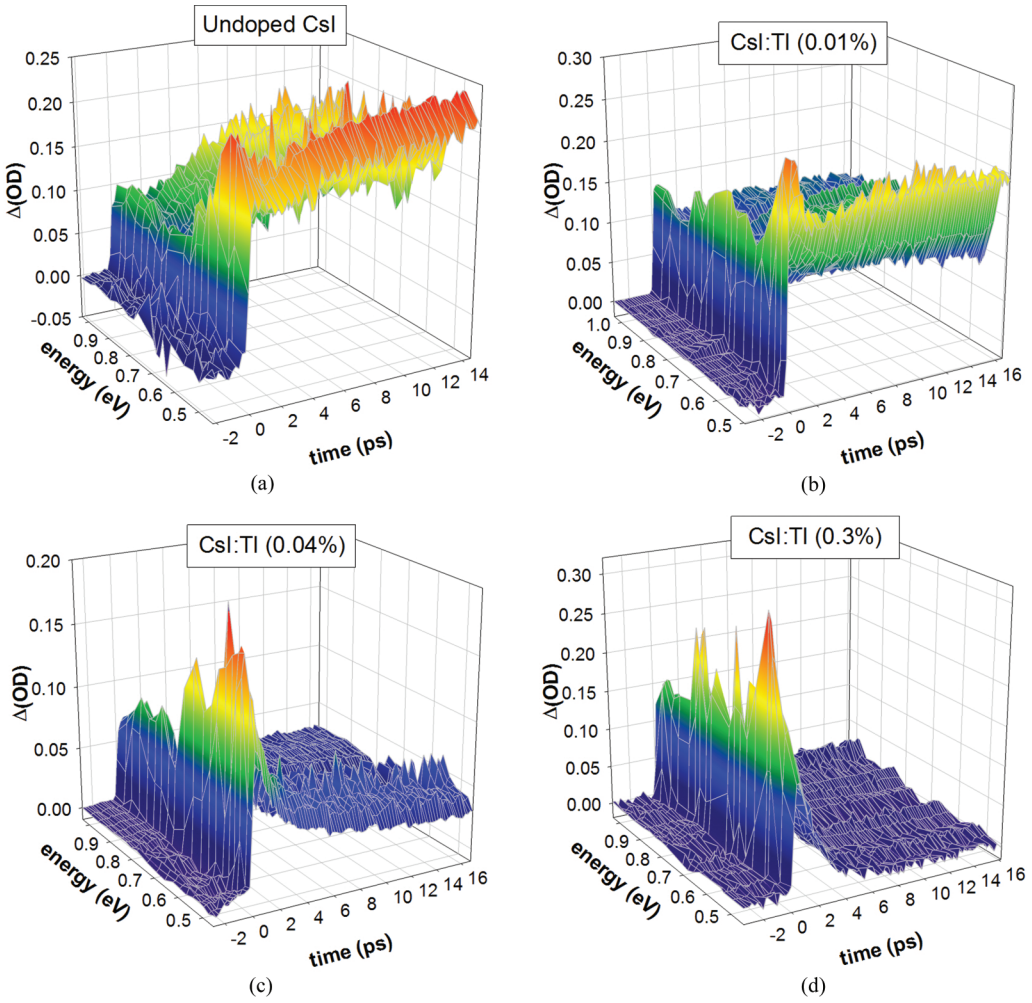

FIG. 2. (Color) Time-resolved infrared absorption spectra induced by interband excitation of undoped CsI, CsI:Tl(0.01%), CsI:Tl(0.04%), and CsI:Tl(0.3%) with $2h\nu = 5.9$ eV are shown in pseudo 3D display format, where time increases left to right and photon energy from 0.45 to 1.0 eV increases from foreground to background.

content in the CsI and NaI samples is about five times lower due to the segregation coefficient. The segregation coefficient for Eu^{2+} in SrI_2 is approximately 1 due to the close size match of Eu^{2+} and Sr^{2+} [25].

III. RESULTS AND DISCUSSION

A. CsI and CsI:Tl

Figure 2 shows time-resolved infrared absorption spectra of undoped CsI, CsI:Tl(0.01%), CsI:Tl(0.04%), and CsI:Tl(0.3%) in pseudo three-dimensional (3D) display format, where time increases left to right and photon energy increases from 0.45 to 1.0 eV from foreground to background. The absorption in Fig. 2 was induced by two-photon interband absorption of a 420-nm (2.95-eV) ps laser pulse of 0.5 ps duration. The amplitude displayed with the help of false color is proportional to the induced change in optical density ($\Delta \log_{10} I_0/I$). The most prominent spectral feature induced by interband excitation in undoped CsI [Fig. 2(a)] is a band with peak at about 0.5 eV photon energy (2480 nm), approaching the long-wavelength limit of our OPA tuning range. There is a second peak at 0.65 eV (1900 nm) which is hidden in the perspective of Fig. 2(a). It can be seen in Fig. 3, which shows the absorption spectrum time averaged

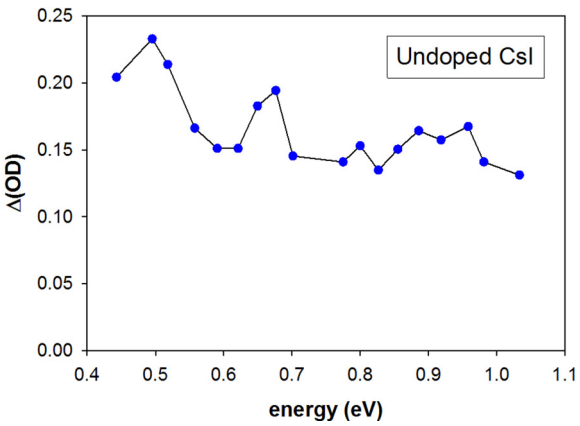

FIG. 3. (Color online) Excitation-induced absorption spectrum in undoped CsI averaged over the time interval 12 to 14 ps after excitation, to better display the two infrared absorption bands at 0.5 and about 0.65 eV.

over the interval 12 to 14 ps in undoped CsI. The 0.7-eV band was the only one visible within the IR continuum spectral range of Ref. [20]. We previously attributed it to the type-II self-trapped exciton (STE) in undoped CsI at room temperature [20], and we continue to assign that identification. Nishimura *et al*. showed that at room temperature the self-trapped exciton (STE) in CsI reaches a thermally equilibriated mixed state of on-center (type-I) and off-center (type-II) STE populations [26].

Based on free-exciton binding energy expected in alkali iodides such as CsI, as well as experiments of Edamatsu *et al*. on type-I absorption spectra in NaI [27], we might expect a type-I STE in CsI to have an absorption band in the 0.3–0.5 eV range. The electronic structure and relaxed lattice configurations of the self-trapped hole (STH) and STE in CsI have been calculated by Van Ginhoven *et al*. [28] using plane-wave pseudopotential density functional theory with Hartree-Fock exact exchange. They find that the STE lattice configuration is similar to the STH, i.e., that the STE is type I. Furthermore, they calculated a lattice relaxation energy of 0.18 eV from the lowest triplet exciton in the unrelaxed lattice to the STE minimum [28]. Comparison of the two-photon absorption spectrum [29] and the one-photon absorption spectrum [30] of CsI indicates the free-exciton binding energy is about 0.25 eV. We suggest that the 0.5-eV induced absorption band in pure CsI arises from the type-I (on-center) component of the room-temperature equilibrated STE population.

Empirical support for assignment of the absorption bands in Fig. 3 to type-I and type-II STEs is found by making a so-called Mollwo-Ivey plot [31,32] of the progression of STE absorption band energies among the structurally similar crystals CsCl, CsBr, and CsI in Fig. 4. Transient absorption bands of type-II STEs in CsCl and CsBr have been measured and identified by Itoh *et al*. [33] and Kravchenko *et al*. [34], respectively. The Mollwo-Ivey plot is based on describing an electron bound to a lattice vacancy with transitions using a particle-in-a-box model, plotting transition energy versus log of the box dimension (nearest-neighbor distance in Fig. 4). A straight-line trend is often found in such plots of F-center [35,36] and STE electron transitions [37], and other bound-

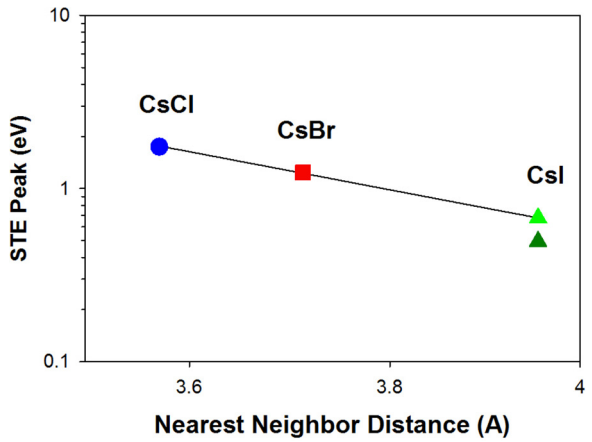

FIG. 4. (Color online) Mollwo-Ivey plot of published STE electron transition energies in CsCl and CsBr and the two infrared absorption peaks in CsI as shown in Fig. 3.

electron centers. Figure 4 shows that such a trend fits the known type-II STE electron transitions in CsCl, CsBr, and the 0.65-eV induced absorption in CsI. The 0.5-eV band falls below the type-II trend line, consistent with it being a type-I STE having less associated lattice relaxation and consequent smaller binding energy of the electron.

The lifetime of the type-I/type-II STE population equilibrated at room temperature in CsI was measured by Nishimura *et al*. [26] to be 15 ns. Our optical delay line could not extend that far, but for the longest delays measured (100 ps), the induced absorption appears constant after the initial transients, and in that sense it is consistent with a 15-ns decay time. The induced infrared absorption appears fully transient in CsI and NaI, recovering before successive pulses at 10 Hz used for the measurement.

Looking at Fig. 2(a) for undoped CsI, the other noticeable feature aside from the STE band is a rapidly rising broad spectrum extending across the full infrared range measured. It will be seen later that it extends up to about 2.5 eV, but not to higher photon energy. Spectrally broad and fast absorption concentrated mainly in the infrared is the typical behavior associated with free-carrier intraband absorption by the photoexcited carrier populations [38]. The spectrum of free-carrier absorption has been well studied in doped semiconductors [39]. The classical Drude prediction of free-electron absorption coefficient is proportional to the number N of free carriers, to the square of the wavelength λ, to the carrier scattering rate $\langle 1/\tau \rangle$, and reciprocally to the effective mass m^*, in the standard case of thermalized free electrons:

$$\alpha \propto \frac{N}{m^*}\lambda^2\left\langle\frac{1}{\tau}\right\rangle \tag{2}$$

and a similar expression for holes. More detailed treatment of different scattering interactions predicts different powers of λ for each scattering contribution to free-carrier absorption: $\lambda^{1.5}$ for acoustic phonons, $\lambda^{2.5}$ for optical phonons, and λ^3 for ionized impurities [40]. Based on the spectral and time signatures, as well as the experiments of Martin *et al*. [14] reviewed in the following, we conclude that free-carrier absorption is responsible for the fast, broad long-wavelength absorption in Fig. 2 and in Figs. 6–9 to be described below. It will also be seen that the phenomenon is quite general, being found also in the spectra of NaI and SrI_2 to be discussed. This is an important point to be established more firmly in continuing work since it underpins the interpretation of these data as giving insight into the interacting populations of free carriers, self-trapped excitons, and trapped carriers in iodide scintillators.

Sugiyama *et al*. [15] and Fujiwara *et al*. [19] observed a broad, fast-growing, and fast-decaying band in alkali bromide and alkali iodide crystals, which they labeled the B band, denoting spectrally broad absorption. It is very likely to be the same phenomenon that appears as the fast and broad initial wall of absorption in our Figs. 2 and 6–10. References [15,19] suggested that the B band was due to vibrationally relaxing self-trapped holes in alkali bromides and iodides doped with electron traps, and vibrationally relaxing self-trapped excitons in pure alkali bromide and iodide crystals.

Martin *et al*. [14] made roughly contemporary measurements of broad optical absorption in alkali halides and SiO_2

that is created promptly upon laser interband excitation and decays in a few picoseconds or less depending on material. They did not measure a complete spectrum to characterize how broad it is, but they found the prompt and fast-decaying absorption upon tuning away from known F-center or self-trapped exciton bands which generally exhibit much longer decay and defined spectral peaks. The fast absorption was in this way identified as a broad background of induced absorption. Significantly, they complemented the optical absorption measurements with time-resolved interferometric phase-shift measurements of refractive index change. They analyzed the induced change in refractive index within a Drude-Lorentz oscillator model, where free conduction electrons are well known to contribute a negative shift to the index. In contrast, bound electrons probed at frequencies below resonance characteristically make a positive shift. They found that the initial optical absorption induced by interband excitation in NaCl, KBr, and SiO_2 was accompanied by a negative excursion of the refractive index which rose and decayed nearly coincident with the broad absorption signal. On this basis, Martin *et al*. identified the fast initial spike of absorption induced by interband excitation as free-carrier absorption, mainly conduction electrons prior to trapping by self-trapped holes or lattice defects [14]. Subsequent trapping of the free electrons by self-trapped holes or defects on picosecond (NaCl, KBr) or subpicosecond (SiO_2) time scales was accompanied by a positive excursion of the refractive index, further confirming the identification of free carriers as the initial absorbing species over a broad spectrum.

In addition to this experimental evidence for attribution of a fast and broad initial spike of absorption in excited insulators to free-carrier absorption, Martin *et al*. presented Monte Carlo simulations of hot electron thermalization time in NaCl and SiO_2, showing that the calculated thermalization time correlated approximately with the observed trapping time of the free electrons [14]. More recently, Wang *et al*. [3,4], Kirkin *et al*. [5], and Li *et al*. [7] have calculated hot electron thermalization and trapping times in alkali iodides, other alkali halides, and oxide crystals establishing that the iodides and other crystals with heavy anions and cations, and thus low optical phonon frequencies, should have the most persistent free carriers. Aside from free-carrier absorption, the free carriers are also manifested physically through the kinetic order of nonlinear quenching in densely excited insulators. As mentioned in the Introduction, Grim *et al*. [1] recently measured the kinetic order of nonlinear quenching in iodide and oxide crystals, finding that iodides such as CsI and SrI_2 display pure third-order quenching due to free-carrier Auger processes, whereas oxides such as BGO (bismuth germinate) and $CdWO_4$ display second-order quenching due to dipole-dipole transfer between self-trapped excitons. It was suggested in Refs. [1,2] that Auger decay dominates in the iodides because the slow thermalization of hot electrons prevents formation of excitons or other trapped electron states throughout the main time of nonlinear quenching. Thus, the early spectrum in picosecond absorption and its rate of conversion to excitons or trapped excitations is closely connected to the nonlinearity and resulting nonproportionality of scintillator response. It seems clear that the dominant kinetic order of nonlinear quenching [1], the B band absorption observed in Refs. [15,19], the fast absorption and phase shifts correlated in Ref. [14], and the broad initial spectrum of excitation-induced picosecond absorption in the present studies of CsI, NaI, and SrI_2 are manifestations of hot free electrons.

The familiar STE peak at 0.5 eV can be seen in the fast initial infrared spectra of heavily doped CsI:Tl in Figs. 2(c) and 2(d), suggesting that some STEs are formed initially in the vibrationally relaxed state. However, the following argument of fractional oscillator strength suggests that the number of such prompt STEs is not large compared to the number of free carriers. Admitting that we presently have a spectral gap in the data from 1.0 up to 2.0 eV, Figs. 2 and 6 together suggest that the broad fast absorption attributed to free carriers extends from below 0.45 eV up to about 2.6 eV. If so, then the additional integrated area under the 0.5-eV STE peak amounts to less than 5% that of the integrated area under the free-carrier spectrum. Based on calculations of the states populated in excitation of BaF_2 by high-energy electrons [41], we have previously remarked that the direct production of excitons in the primary electron stopping event (e.g., evaluated at 0.04 fs) accounts for only about 2% of total excitations [2]. The experimental picosecond absorption spectrum is reasonably consistent with this expectation, and would become even closer if we take into account that free-carrier absorption would continue rising into the infrared below the 0.45-eV spectral limit of our experiment.

The initial spike of directly created excitons coexists in time with the hot free carriers and could be susceptible to ionization by collision with them. This might explain why the initial STE peak in Figs. 2(a), 2(b), and 5 decays in about 1.2 ps before new STEs begin to be created by mutual capture of thermalized free carriers. It should also be kept in mind that the initial STE peak around 0.5 eV rides on top of the spectrally broad free-carrier absorption, and will appear to decay as the free-carrier component under it also decays in a few picoseconds.

Now, look at the effect on induced infrared absorption of adding Tl ions to CsI, shown in Figs 2(b)–2(d). The broad and fast free-carrier spectrum is still induced, but it drops away to very low values everywhere in the 0.45–1.0 eV infrared spectrum after a few picoseconds for the two heavier Tl dopings. It drops faster and farther for higher Tl concentration. In the lightly doped 0.01% Tl sample shown in Fig. 2(b), the initial peak drops somewhat faster and farther than in pure CsI, before the slower (∼4 ps) regrowth of the STE band at 0.5 eV starts. The 0.5-eV band can be seen to decay again after about 10 ps for 0.01% Tl. This is seen more clearly in Fig. 5(a), comparing the 0.5-eV absorption over a 17-ps range for all four Tl doping levels in CsI. Figure 5(b) plots 0.78-eV absorption in CsI:Tl(0.01%) over the full 100-ps range of our optical delay stage, along with a fit to the two rising and falling populations.

According to previously established understanding of hole and electron trapping in CsI:Tl, the initially free holes are self-trapped very quickly in the host lattice, and many of the initially free electrons are trapped on the Tl^+ dopant as Tl^0. The rapid disappearance of initial free-carrier absorption with no STE bands growing in to replace it in Figs. 2(c) and 2(d) seems at first to suggest that the Tl dopants have destroyed excited states available for luminescence. Of course, this can not be the case since at room temperature, CsI:Tl has significantly higher

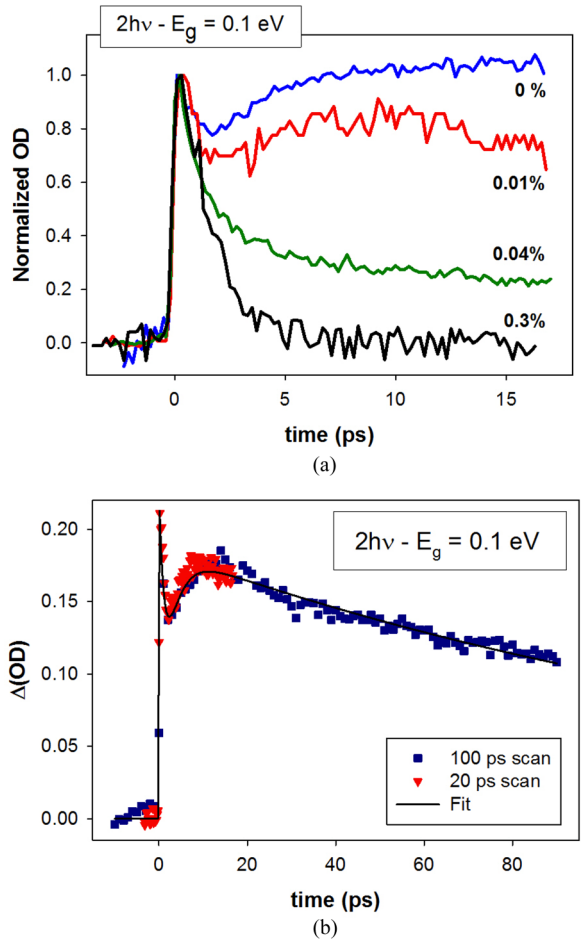

FIG. 5. (Color online) (a) Compares normalized 0.5-eV absorption over a 17-ps range for all four Tl doping levels in CsI. (b) Displays and fits the two stages of rise and fall of 0.78-eV induced infrared absorption in lightly doped (0.01% Tl) CsI at room temperature. The initial decay constant is 1.23 ps. The slower rise and decay constants are 2.74 and 167 ps, respectively.

light yield than undoped CsI. Clearly what has happened is that trapping of electrons on Tl moves absorption oscillator strength out of the infrared (where absorption is primarily attributable to free carriers and self-trapped excitons), and into some other part of the spectrum. Looking at Fig. 6 shows that the visible spectrum is where much of the oscillator strength of induced absorption was moved upon Tl doping.

The visible spectrum of induced absorption from 2.0 to 3.6 eV is shown for undoped CsI and three Tl dopings of 0.01%, 0.04%, and 0.3% respectively in Figs. 6(a)–6(d). Undoped CsI in Fig. 6(a) exhibits almost no persistent absorption in the visible range. The only substantial absorption is the fast rising and decaying absorption below 2.6 eV. In line with the discussion of Fig. 2, we suggest that it is the high-photon-energy limit of free-carrier absorption. There is a weak persistent absorption band at about 2.3 eV in undoped CsI. We tentatively attribute it to the $\sigma_u - \sigma_g$ hole transition of the STE in these room-temperature experiments. Observation of a 3.4-eV induced absorption band in CsI has been reported in Refs. [20,42]. Surprisingly, a 3.4-eV band is not observed in Fig. 6(a) for undoped CsI, but it is indicated in Fig. 6(b) for 0.01% Tl in CsI. Note that there is no free-carrier absorption at 3.4 eV in Fig. 6 because the wavelength is too short in view of Eq. (2). Instead, the 3.4-eV band in Fig. 6(b) appears by itself after a delayed growth.

Figures 6(b)–6(d) show that adding Tl dopant introduces a persistent broad absorption spectrum with peak near 2.5 eV. In this optical delay-line experiment conducted at 10-Hz repetition rate, persistent implies a decay time less than 0.1 s but much longer than 60 ps. The initial free-carrier absorption is apparent up through 0.04% Tl, but it becomes only a shoulder on the rising 2.5-eV band at 0.3% Tl doping. It should be noted that the visible data of Fig. 6 were measured using third-harmonic laser light exciting states at $2h\nu = 8.86$ eV, whereas the infrared data of Fig. 2 were measured with second-harmonic, exciting states at $2h\nu = 5.9$ eV. This was dictated by experimental considerations of keeping the blue second-harmonic pump beam out of the detector, but it means that the initial carrier energies above the cbm were different in Figs. 2 and 6.

Pursuant to our knowledge that self-trapped holes (STH) and electrons trapped on thallium (Tl^0) should be present on this time scale after excitation of CsI:Tl, and should represent roughly the same integrated oscillator strength as the initial free-carrier absorption, it seems reasonable to tentatively attribute the broad 2.5-eV absorption to a combination of STH and Tl^0 absorption. Sidler *et al.* [43] observed two absorption bands attributable to Tl^0 in CsI:Tl at low temperature after irradiation: at 620 nm (2 eV) and 500 nm (2.5 eV). The attribution to Tl^0 is suggested because these two bands were found in irradiated CsI:Tl but not in CsI:Na. In addition, they observed a stronger band at 410 nm (3.05 eV) attributed to the STH in both CsI:Tl and CsI:Na at 4 K. Since we do not see a peak of any kind at 3 eV in Fig. 6, but feel sure that there should be STH absorption in the Tl-doped samples, we surmise that the STH absorption band shifts from 3 eV at $T = 4$ K to about 2.5 eV at room temperature. This is at least qualitatively consistent with the fact that the STH is becoming mobile at room temperature and so occupies vibrational states that are less strongly relaxed and have smaller $\sigma_u - \sigma_g$ molecular orbital splitting. The Tl^0 bands may not have such a strong temperature dependence, so it may be considered that the 2.5-eV transient absorption observed at room temperature in our experiment is a composite of both STH and Tl^0 absorption. Performing low-temperature ps absorption spectroscopy in the future will help clarify this assignment.

Yakovlev *et al.* [44] list transition energies of Tl^0 in CsI:Tl. The $6^2P_{1/2} \rightarrow 6^2D_{3/2}$ band has been reported at 2.14 [45] and 2.25 eV [44]. The $6^2P_{1/2} \rightarrow 6^2P_{3/2}$ band has been reported at 1.31 [45] and 1.36 eV [46], but the $6^2P_{1/2} \rightarrow 6^2P_{3/2}$ transition is in the 1 to 2 eV spectral gap of our current measurements. According to Yakovlev *et al.* [47], the Tl^0 level is approximately mid-gap in CsI:Tl. All of the above reports would be consistent with observing the $6^2P_{1/2} \rightarrow 6^2P_{3/2}$ transition as part of the 2.5-eV band in Figs. 6(c) and 6(d).

Taking a summary view of Figs. 2 and 6 together, it is striking how the oscillator strength of induced absorption shifts from the infrared in undoped CsI to the visible in Tl-doped CsI. This is a direct visualization of energy storage in the doped scintillator, and as such these data can be used to deduce the trapping rates on energy storage sites.

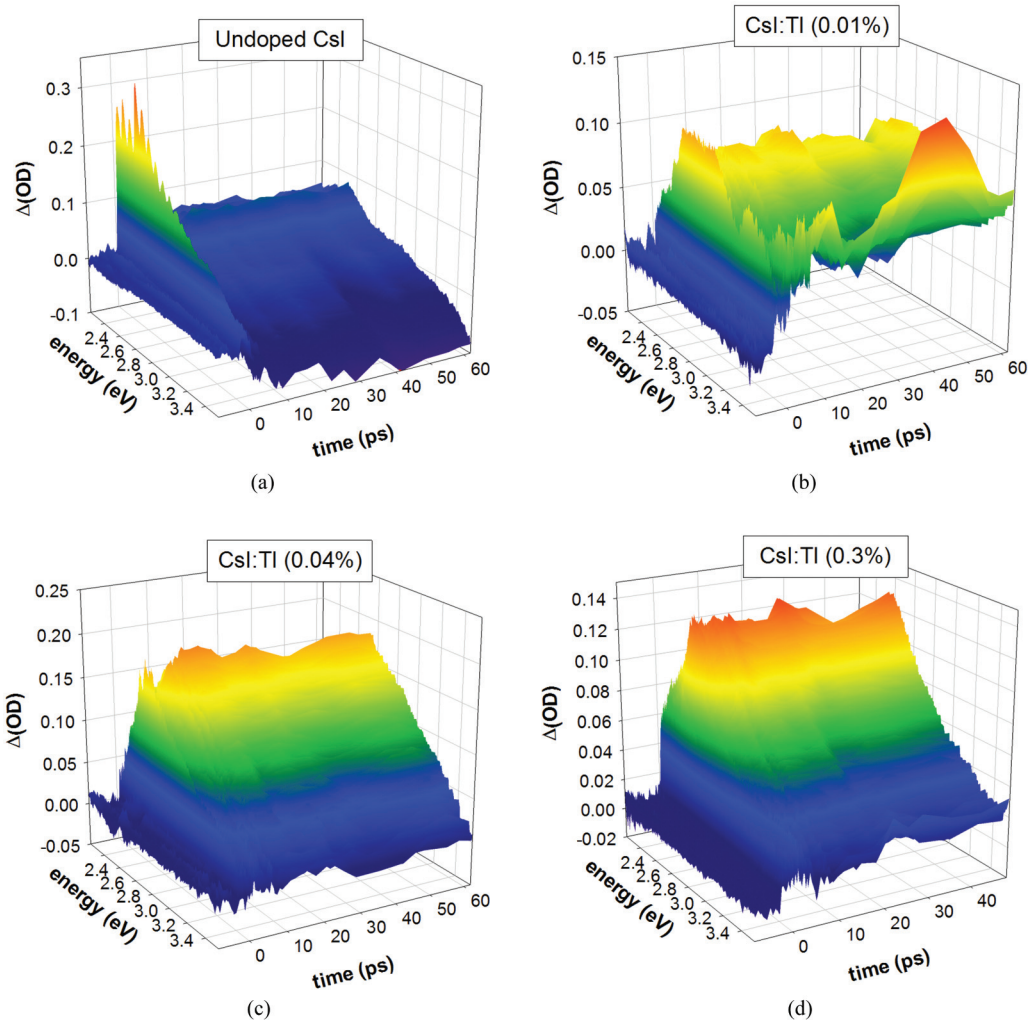

FIG. 6. (Color) Visible absorption spectra induced by $2h\nu = 8.86$ eV excitation in undoped CsI and CsI:Tl (0.01%, 0.04%, and 0.3%) at room temperature.

B. NaI and NaI:Tl

Figures 7 and 8 present a similar study of absorption induced by interband absorption in NaI and NaI:Tl for the infrared spectrum (Fig. 7) and the visible spectrum (Fig. 8). For NaI:Tl, we had only one doping level: 0.1% Tl. The infrared spectra for undoped and doped NaI show the broad and fast spectrum very similar to CsI, which we have attributed to free carriers. Undoped NaI in Fig. 7(a) exhibits an absorption band with persistence of at least 15 ps near 0.5 eV. It is weak compared to the similar feature in CsI, which could be consistent with only catching the beginning of absorption rising to a peak below 0.5 eV as was found for the STE in NaI by Edamatsu *et al.* [27]. The known type-I STE absorption band has its peak at or below 0.25 eV in NaI at low temperature, but the high-energy tail of this absorption extends to 0.6 eV even at $T = 4$ K [27]. Anticipating a shift and broadening of the absorption band from 4 K to room temperature, the spectrum in Fig. 7(b) is at least consistent with how the NaI STE infrared absorption may appear in the spectral range near 0.5 eV. As in CsI, the short-lived initial spectrum attributed mainly to broad free-carrier absorption includes a peak at the position of the STE band, but the exciton peak comprises a small fraction of the total free-carrier absorption oscillator strength as can be seen upon performing the integral over spectrum. When Tl doping is added in Fig. 7(b), the spectrum looks very similar except that the tail of STE absorption at 0.5 eV decays rather than remaining persistent on the 15-ps time scale. The visible spectra of NaI and NaI:Tl in Figs. 8(a) and 8(b) bear an interesting resemblance to the visible spectra of CsI and CsI:Tl in Fig. 6. In particular, the fast absorption attributed to free carriers extends from low energy to about 2.5 eV and then drops off toward 2.8 eV. This consistent behavior in both infrared and visible ranges for two separate hosts builds confidence in a universal occurrence of free carriers in the earliest spectrum. There is a persistent (15-ps) band of significant strength at 2.45 eV in NaI:Tl(0.1%), very reminiscent of the 2.5-eV band in CsI:Tl. For reasons similar to those discussed for CsI:Tl, we tentatively attribute the 2.45-eV band in NaI:Tl to combined STH absorption and Tl^0 absorption at room temperature. The persistent 2.35-eV absorption in undoped NaI [Fig. 8(a)] is suggested to be the $\sigma_u - \sigma_g$ hole transition of the STE in NaI, taking into account spectral shifts at room temperature relative to known NaI STE transitions at low temperature [12,48]. Parallel spectral features in the

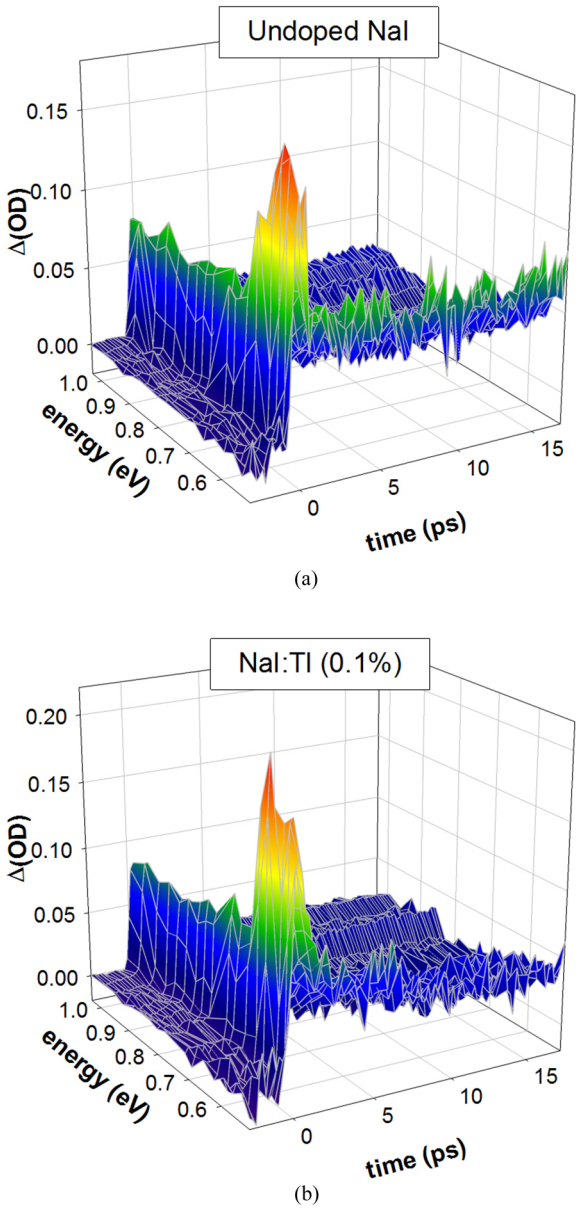

FIG. 7. (Color online) Infrared absorption spectra induced by $2h\nu = 8.86$ eV excitation in (a) undoped NaI and (b) NaI:Tl (0.1%) at room temperature.

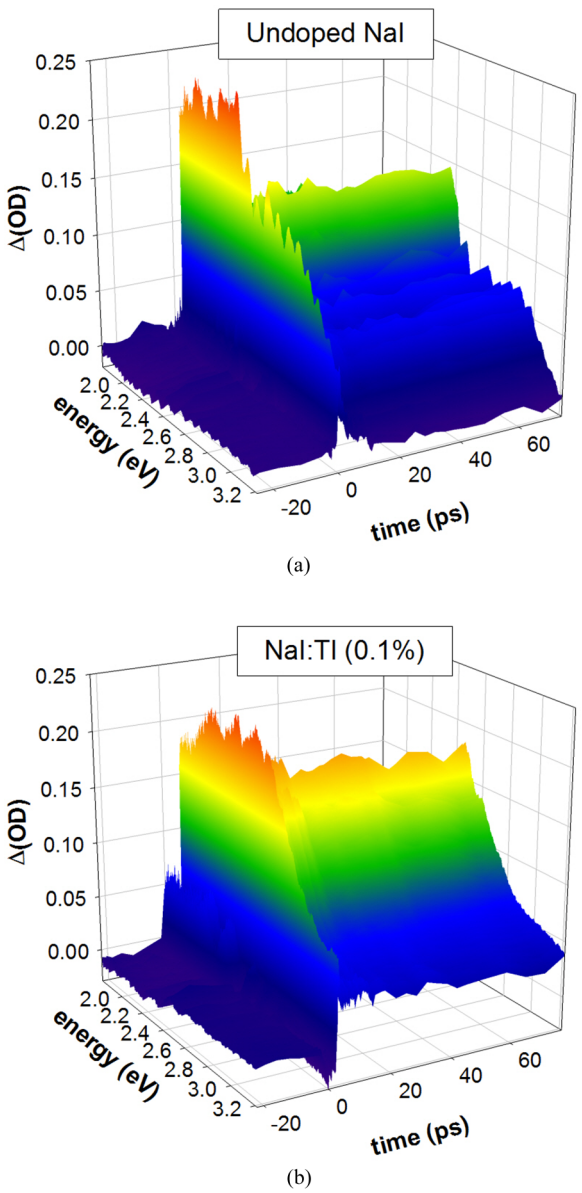

FIG. 8. (Color online) Visible absorption spectra induced by $2h\nu = 8.86$ eV excitation in (a) undoped NaI and (b) NaI:Tl (0.1%) at room temperature.

early-time spectra of CsI and NaI are reassuring about common origins.

C. SrI_2 and SrI_2:Eu

Figures 9(a) and 9(b) show infrared spectra of excitation-induced absorption at room temperature in undoped SrI_2 and SrI_2:Eu(3%), respectively, measured in a similar way as Figs. 2 and 7. The fast initial absorption behaves in many respects like the similar feature attributed to free-carrier absorption in CsI and NaI. It rises and falls in a few picoseconds and it extends through much of the infrared and visible ranges measured, terminating on the high-energy end between 2.5 and 2.8 eV. At the low-energy infrared end, it seems less strong than in CsI and NaI, but this appears the only major difference. Overall, the constancy of this feature in the three materials measured in this work contributes to our confidence in assigning the universal phenomenon of free-carrier absorption in these iodides.

As we have noted above, existence of STEs in SrI_2 is predicted by recent density functional theory (DFT) calculations [49]. Luminescence attributed to STEs has been reported at 3.1 eV for $T = 295$ K [50,51] and at 3.4 eV for $T < 100$ K, above which thermal quenching was observed [23,52]. The fact that quenching of STE luminescence above 100 K was observed in Refs. [23,52] but not in Refs. [50,51] might be associated with the experimental circumstance that the excitation was near the surface in Refs. [23,52] (ultraviolet on crystal, x-ray on powder) but deeper in Refs. [50,51] (1-MeV electrons on crystal). That is, the observed quenching could be thermally activated mobility rather than crossing to the ground

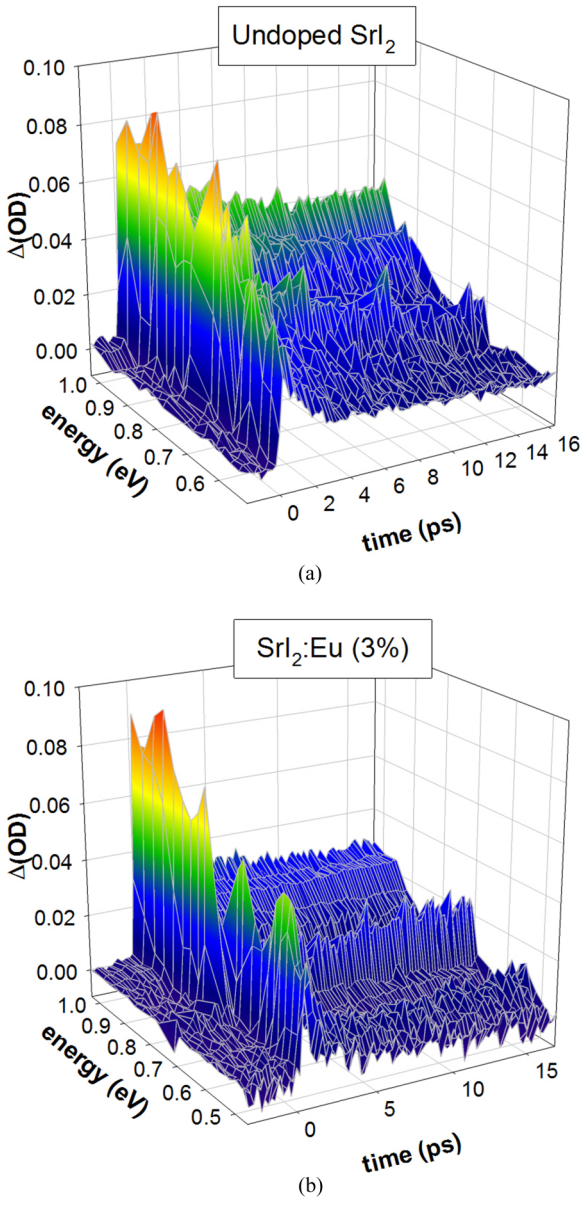

FIG. 9. (Color online) Infrared absorption spectra induced by $2h\nu = 5.9$ eV excitation in (a) undoped SrI_2 and (b) SrI_2:Eu(3%) at room temperature.

state. Based on calculations [49] and luminescence [50,51], the STE should be observable in the absorption spectra of excited SrI_2 at room temperature.

Very little persistent infrared absorption (on the 15-ps time scale) in undoped SrI_2 is found in the 0.5 to 0.8 eV range of a strength corresponding to the STE bands in CsI and NaI. Certainly, there is nothing throughout the infrared range measured that can compare with the STE in CsI. By default of not seeing strong STE absorption bands in undoped SrI_2 below 1 eV and above 2 eV, the spectral gap for 1 to 2 eV in our present experiments is suspected as a likely location to find them. The apparent tails of absorption bands near 1 eV in Fig. 9(a) and near 2 eV in Fig. 10(a) are thus suggestive of STE absorption bands due to electron transitions and hole transitions, respectively.

Although the existence of the STE and its luminescence transitions in SrI_2 have been predicted from first-principles electronic-structure calculations [49], the absorption spectra have not been calculated. Rough guidance on absorption energies of the hole and electron components of an STE in SrI_2 may be estimated from the energies of the STE hole and electron states relative to their respective band edges in the DFT hybrid functional calculations [49]. Li *et al.* have estimated the F-center absorption band energy in SrI_2 from hybrid functional DFT calculation of the F to F^+ optical ionization and an empirical scaling of the F absorption transition energy relative to its ionization limit, finding 1.67 eV [36]. This should represent an upper limit (extreme type-III relaxation) for the main electron band in optical absorption of STEs [48]. The ~1-eV infrared and 2-eV visible transient bands in undoped SrI_2 are tentatively suggested as possibilities for the electron and hole transitions, respectively, of the STE in SrI_2.

The 1-eV absorption in Fig. 9(a) appears to be the low-energy shoulder of a candidate STE absorption band somewhat above the 1-eV limit of our present infrared spectra. There are two other weaker bands at 0.9 and 0.7 eV that have a persistence also possibly consistent with an STE. The 0.7-eV persistent band grows stronger in the 3% Eu-doped sample [Fig. 9(b)], so we guess that it may be more likely associated with Eu than the STE.

Figures 10(a)–10(d) show visible spectra of excitation-induced absorption at room temperature in undoped SrI_2 and three concentrations of Eu doping, 0.2%, 0.5%, and 3%, respectively. The visible spectral range from 2 to 3.1 eV exhibits substantially more induced absorption for both undoped and Eu-doped SrI_2 compared to the infrared. In undoped SrI_2 there are induced absorption bands of at least 70-ps persistence occurring roughly around 2 and 2.9 eV, which might be due to hole transitions of the STE or the STH. Adding Eu dopant to SrI_2 leads to an excitation-induced absorption band near 2.25 eV, clearly different from the 2-eV band in undoped SrI_2. At 3% Eu, the excitation-induced absorption includes a plateau extending through much of the visible spectrum above the 2.25-eV peak.

Figure 11 compares the decay time of 1-eV absorption in undoped and 3% Eu-doped SrI_2. There is a 1.4-ps decay component in undoped SrI_2 followed by leveling off in a long-lived absorption. For 3% Eu doping, Fig. 10 shows that the initial decay of absorption becomes remarkably fast, i.e., 0.8 ps including the convolved 0.5-ps pulse width. If this accelerated drop in free-carrier absorption is due to capture on Eu^{2+}, it is remarkably faster than electron capture processes we deduced in the previous sections on CsI:Tl and NaI:Tl. Part of the reason is that 3% doping of Eu^{2+} in SrI_2 is at least 70 times higher concentration than the maximum Tl^+ concentration in our samples of the alkali halides. The apparent subpicosecond capture time of free carriers on Eu^{2+} in SrI_2 presses the limits of hot free-electron cooling and capture time that we have invoked to explain the pure third-order quenching observed in SrI_2 [1]. Further work will seek to reconcile the two experiments and decide if the higher concentration of Eu in SrI_2 is mainly responsible, or if Eu has an inherently faster trapping rate.

In the first place, we should note that Tl^+ in the alkali halides can trap both electrons and holes forming Tl^0 and

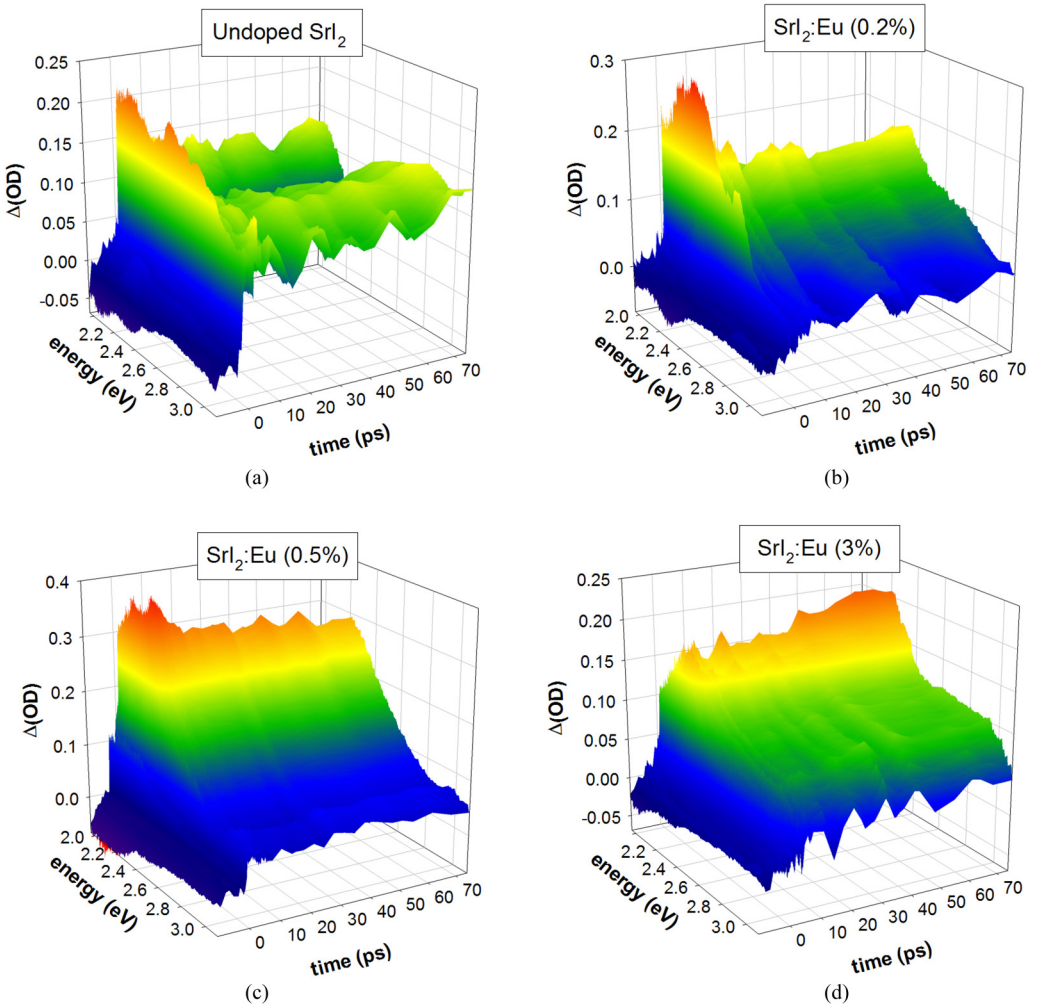

FIG. 10. (Color online) Visible absorption spectra induced by $2h\nu = 8.86$ eV excitation in undoped SrI_2 and SrI_2:Eu(0.2%, 0.5%, and 3%) at room temperature.

Tl^{++}, respectively, and Tl^{+*} when on the same ion. Due to the very small mobility of self-trapped holes in the alkali halides, Tl^{+} functions mainly as an electron trap in the picosecond time range that we are probing. On the other hand, Eu^{2+} in

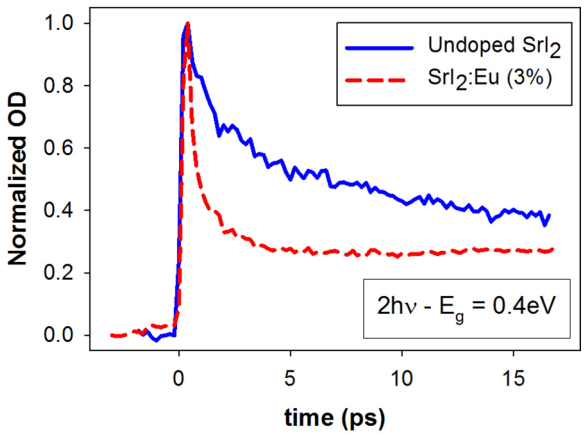

FIG. 11. (Color online) Time dependence of induced absorption in undoped SrI_2 and SrI_2:Eu(3%) at 1 eV when the excitation populates states 0.4 eV above the band gap.

SrI_2 is believed to function initially as a hole trap and then to Coulombically attract an electron after the hole is trapped. Since holes also self-trap in SrI_2, the ability to dope with Eu^{2+} to percent levels should be important in this case. Taking Tl segregation coefficient into account, the actual mole % doping level in our nominal 0.3 wt % Tl:CsI sample is about 0.042 mole %, to be compared to our 0.2 mole % Eu:SrI_2 sample. Comparing rise times of the visible absorption spectra attributable to charges trapped on activators in SrI_2:Eu(0.2%) [Fig. 10(b)] and CsI:Tl(0.3%) [Fig. 6(d)], the rough conclusion is that Tl is comparable to Eu in its ability to trap charge in states responsible for visible absorption in the two hosts. This is a rough comparison, but it points initially toward the higher achievable activator concentration in SrI_2:Eu as a main factor in the remarkably fast capture of carriers evidenced in Fig. 11.

In all of the spectra displayed in this paper for CsI, NaI, and SrI_2, there is consistently found a fast-rising and fast-decaying broad absorption band from infrared to mid-visible. We have attributed it to free-carrier absorption, and free carriers are central to the nonlinearity of light yield in heavy halides [2]. It is therefore important to be sure that this feature is not an artifact due, e.g., to two-photon absorption of coincident pump and probe photons (pump/probe TPA) [53]. A diagnostic to

check for this artifact is to change the pump photon energy as we have done in this study, and see if an absorption peak moves corresponding to the shift in pump photon energy. There was found no significant feature which behaves in that way within the present probe spectral ranges. When using 2.95-eV pump photons, the onset of possible TPA probe photon absorption would be $E_g - 2.95\,\text{eV} \sim 3\,\text{eV}$ in CsI and NaI. The infrared and most of the visible spectrum are therefore free of pump/probe TPA for the 2.95-eV pump beam. This establishes that the fast and broad initial absorption we have seen is not a pump/probe TPA artifact in any of the three iodide materials in this study.

D. Hot electron cooling and capture, exciton formation, and trapping on dopants

Figure 12 displays absorption at 1 eV in CsI with and without Tl doping versus time after excitation. The measurements were made for two different values of $2h\nu - E_g$, the energy of the initially excited electron-hole pair state in excess of the band gap. The photon energy of the pump beam which is two-photon absorbed in the sample is $h\nu$, selectable as second harmonic (2.95 eV) and third harmonic (4.43 eV) of the laser fundamental. In Fig. 12(a), the initially excited carriers in CsI

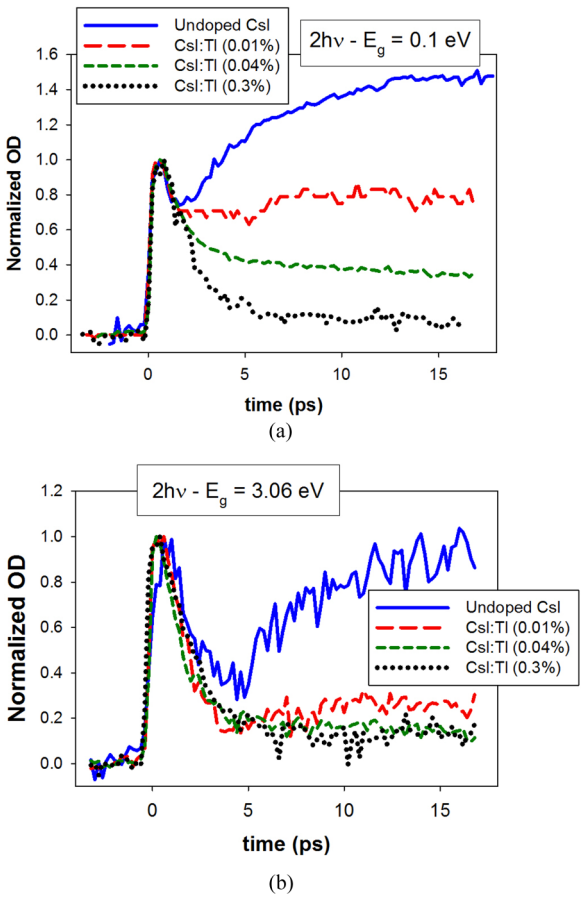

FIG. 12. (Color online) Induced absorption versus time at 1 eV for undoped and Tl-doped CsI samples when the initial excitation creates carriers (a) only ~0.1 eV above the band gap or (b) 3 eV above the band gap.

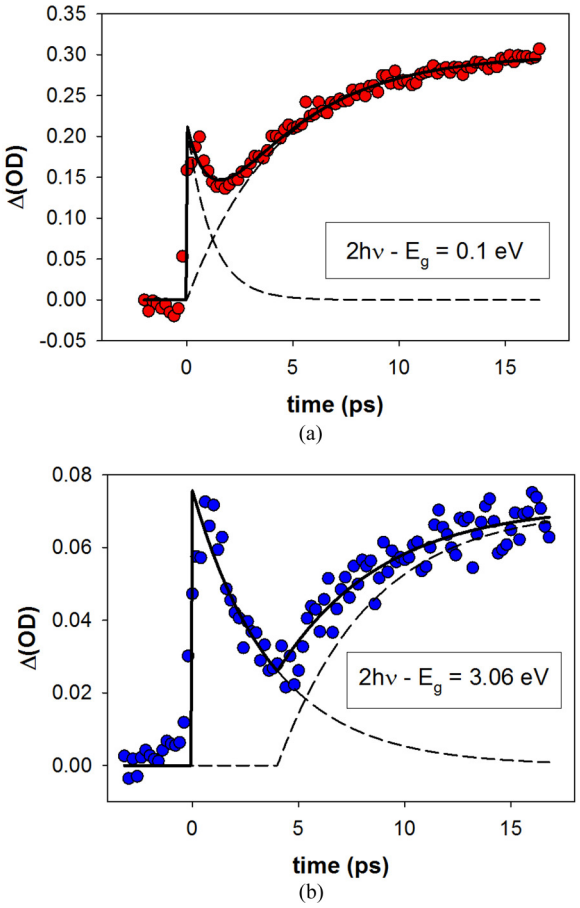

FIG. 13. (Color online) The 1-eV absorption data for undoped CsI from Fig. 12 have been fit to the functions given in Eqs. (3) and (4) for excess initial carrier energies of 0.1 and 3.06 eV, respectively.

start out almost thermalized, sharing excess energy of about 0.1 eV above the 5.8-eV band gap. In Fig. 12(b), the initially excited carriers are quite hot, sharing excess energy of 3.06 eV. Based on the spectra and discussion in Sec. III A, we have associated the initial spike of absorption at 1 eV with free carriers, and the slower rise of absorption in undoped CsI with self-trapped excitons. Figure 12 shows the conversion from free carriers to STEs moving to later time as the initial excited electron energy becomes higher. The STE growth time seems to remain about the same, but to start later with respect to the free-carrier spike when the excitation energy is higher.

In Fig. 13, the data for undoped CsI at 1 eV have been fit to exponential decay of the free-carrier component and saturating exponential growth of the STE component starting after a delay.

The fitting function for $2h\nu - E_g = 0.1$ eV is

$$y = ae^{-bt} + c(1 - e^{-dt}) \quad \text{for} \quad t > 0, \tag{3}$$

where $1/b = 1.15$ ps and $1/d = 4.31$ ps. The fitting function for $2h\nu - E_g = 3.06$ eV is

$$y = \begin{cases} ae^{-bt} & \text{for} \quad 0 < t < 4, \\ ae^{-bt} + c(1 - e^{-d(t-4)}) & \text{for} \quad t > 4, \end{cases} \tag{4}$$

where $1/b = 3.75$ ps and $1/d = 4.42$ ps and the thermalization time (onset of electron capture) = 4 ps.

The 4-ps delay before the onset of the slower growing absorption found for $2h\nu - E_g = 3.06$ eV is in reasonable agreement with the calculation of hot electron cooling time and subsequent time to capture on self-trapped holes by Li *et al.* [2,7], starting from initial hot electron energy of 5 eV. The criterion for capture was that the electron should have cooled sufficiently that the next optical phonon scattering event with energy loss could reach an energy 3 kT below the conduction band edge in the local potential of the hole or activator. The thermalization time is consistent with published simulations of hot electron cooling and capture by Wang *et al.* [3,4]. Kerisit *et al.* have recently performed Monte Carlo simulations of hot electron cooling and capture on holes in CsI for precisely the two initial energy conditions of the experiments in Fig. 12, finding good agreement of the simulated and experimental capture times under the capture criterion stated above [8]. This experiment can be interpreted as providing a direct view of electron thermalization as a function of the initial hot electron energy, and its role in delaying exciton formation. It is complementary to the recent study by Belsky *et al.* [54] analyzing Ce^{3+} light yield in $LiYF_4$:Ce crystals upon ionizing the Ce^{3+} directly with tunable synchrotron radiation. From analysis of light yield and formation-decay kinetics, they could deduce the thermalization length as a function of hot electron excitation energy above the Ce4$f \rightarrow$Y4d and Ce4$f \rightarrow$Li2p thresholds.

Figure 14 shows the production and decay of the peak of visible absorption (2.5 eV) in CsI and CsI:Tl. The growth of the 2.5-eV absorption we have attributed to a combination of STH and Tl^0 goes to completion in about 3 ps in CsI:Tl(0.3%). There is an interesting qualitative resemblance of Fig. 14 to the infrared data in Fig. 12, except that the dependence on Tl doping is inverted. This is again consistent with energy storage on Tl^0 and STH moving oscillator strength from the infrared to the visible spectrum. The intermediate Tl concentrations in Fig. 14 indicate a trapping time of order 3 ps for electrons on Tl^0, which is consistent with interpreting the 2.5-eV band as more strongly representative of Tl^0 than of STH. At 0.3% Tl by weight (423 ppm), or a volume concentration of 2.55×10^{20} Tl^+/cm^3, the visible absorption rises noticeably faster than the infrared STE absorption seen in Fig. 12. This Tl^+ concentration is at least two orders of magnitude higher than the hole concentration produced by two-photon absorption in this experiment.

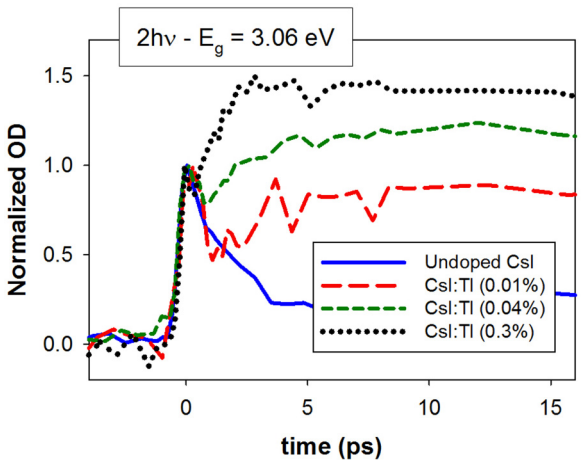

FIG. 14. (Color online) Production and decay of the peak of visible absorption (2.5 eV) in CsI and CsI:Tl.

It will be noticed that in Fig. 14, the initial carrier energy is 3.06 eV in excess of the band gap, but there is not a 4-ps thermalization delay before the onset of growth of visible absorption, in contrast to the infrared absorption presumably of the STE in Fig. 13. The compelling evidence for a 4-ps thermalization delay before onset of electron capture on the self-trapped hole in Fig. 13 seems not warranted for the visible absorption attributed mostly to Tl^0. The ability to capture hot electrons seems to be much greater for Tl^+ than for the self-trapped hole. The STH in CsI is a shallow electron trap (~0.7 eV for type-I STE relaxation) whereas recent studies indicate that Tl^0 is a fairly deeply trapped electron in CsI, about 2 eV below the conduction band minimum [47]. The electron is believed to diffuse by tunneling in the Tl subband [47]. Recent first-principles calculations of carrier capture rates [21] have suggested to us that traps of different depth and different linear coupling to local phonon modes can have significantly different hot carrier capture rates. This will be explored computationally and experimentally in future studies. Without some significant variability of hot capture rates on different traps, Figs. 13 and 14 seem difficult to reconcile.

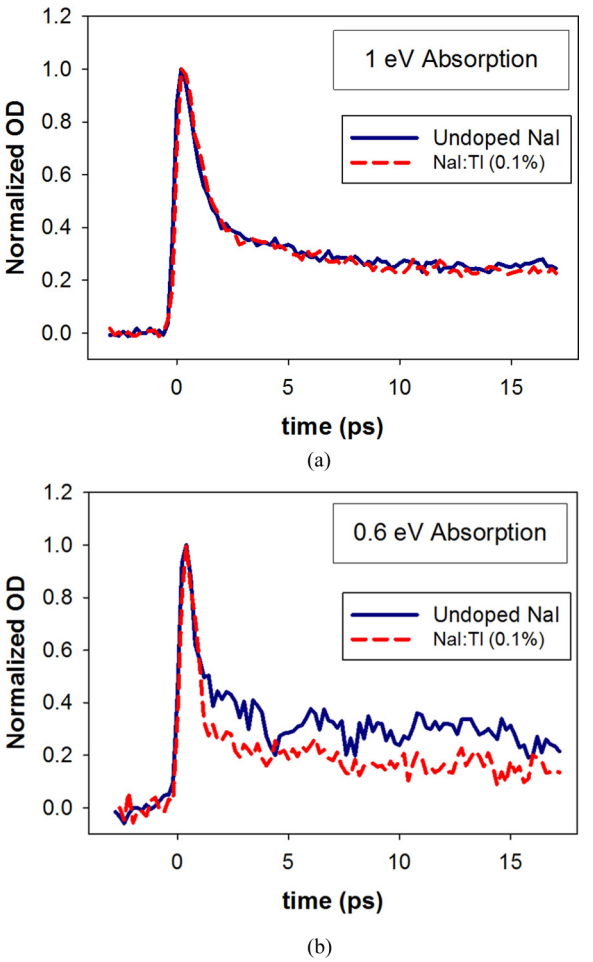

FIG. 15. (Color online) (a) Shows 1-eV absorption rise and decay in NaI and NaI:Tl induced by 8.86-eV excitation. (b) Shows a similar set of data for absorption at 0.6 eV induced by 8.86-eV excitation.

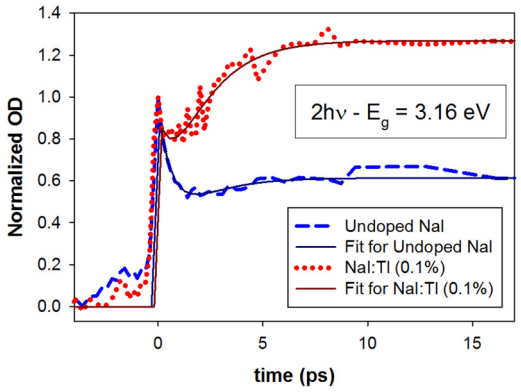

FIG. 16. (Color online) Visible absorption near 2.5 eV induced in NaI and NaI:Tl by 8.86-eV excitation.

Figure 15(a) shows 1-eV absorption rise and decay in NaI and NaI:Tl. This photon energy is not at a known absorption transition of the STE nor of Tl^0, so it mainly shows the rise, and the decay due to cooling and trapping, of free-carrier absorption, settling to a residual 30% absorption of unknown origin. The behavior is nearly identical in undoped and Tl doped NaI. Figure 15(b) shows a similar set of data for absorption at 0.6 eV, which may include a tail of the infrared STE absorption in NaI.

Figure 16 shows the time dependence of visible absorption near 2.5 eV induced in NaI and NaI:Tl by 8.86-eV excitation. Similar to CsI, after initial free-carrier absorption, the band attributed to Tl^0 and STH in NaI:Tl grows in about 1.75 ps as fitted to Eq. (3) with $1/b = 0.81$ ps and $1/d = 1.75$ ps.

Figure 17 shows time dependence of absorption induced by by 8.86-eV excitation in undoped and Eu-doped SrI_2 measured at the peak of induced visible absorption near 2.3 eV.

A spike of free-carrier absorption appears resolvable in the undoped and 0.2% Eu-doped samples. In the more heavily doped samples, transfer from free carriers to Eu dopant appears to be so fast that free carriers can not be resolved as a separate

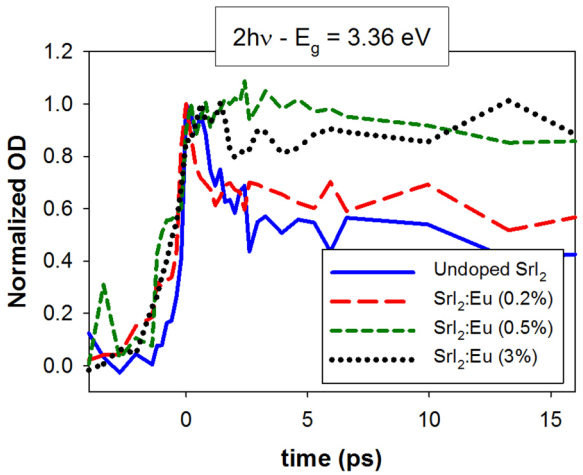

FIG. 17. (Color online) Time dependence of absorption induced by 8.86-eV excitation in SrI_2 and SrI_2:Eu measured at the peak of induced visible absorption near 2.3 eV.

population at this wavelength. Recall that a similar conclusion was suggested by the visible spectra for SrI_2:Eu in Fig. 10.

IV. CONCLUSIONS

Fast, spectrally broad absorption attributable to free carriers is observed in all three metal iodides studied. Since holes are self-trapped in all three of these metal iodide crystals, we specifically attribute the fast, broad, red/infrared absorption to conduction electrons. On the basis of Refs. [1–5] and Fig. 13, an important reason for the electrons remaining free for one to several picoseconds (depending on initial excitation energy) is the hot electron thermalization time mediated by the optical phonon frequency. Figure 13 provides a direct experimental view of the dependence of electron thermalization and capture time (on an STH to form STE) upon initially excited hot electron energy.

The free-carrier absorption is replaced in a few picoseconds or less by other species as the free electrons thermalize and become trapped. In undoped CsI, peaks attributable to type-I (0.5-eV) and type-II (0.7-eV) self-trapped excitons grow with a 4-ps time constant. In NaI, the STE is purely type I with its main electron transition somewhat below our 0.45-eV spectral limit [27], but even so, Fig. 7 appears to capture the high-energy tail of the type-I STE in NaI. There is a time offset in the beginning of STE growth, depending on the excess energy of initially excited carriers above the band gap. The time delay before pairing of electrons and holes begins is observed to be about 4 ps when the initial excitation energy is 3 eV above E_g in CsI. This is in rather good agreement with Monte Carlo simulations of hot electron thermalization and capture in CsI [3,4,7,8], as compared in Ref. [2]. Adding Tl to CsI kills the slow (∼4 ps) growth of self-trapped excitons in favor of visible bands suggested to arise from Tl^0 and STH.

CsI:Tl and NaI:Tl are similar in exhibiting transfer of dominant oscillator strength from the infrared transitions of STE in undoped material to the visible transitions of combined STH and activator-trapped electrons in Tl-doped material. This is a visualization of energy storage on spatially separated traps (Tl^0 and STH) that limits the duration of Auger quenching. SrI_2 appears similar in the visible transitions of the dopant (and possibly STH) but the absorption strength of undoped SrI_2 in the infrared is comparatively weaker. There is currently a gap in our spectral coverage from 1 to 2 eV for technical reasons. The SrI_2 data around 1 eV suggest that there may be a band of induced absorption somewhat above 1 eV, allowing this as a possibility for where a strong STE absorption band might yet be found in SrI_2.

The STE absorption in CsI has a “double-dip” time signature. Absorption with the spectral signature of type-I STE is initially created along with free-carrier absorption, and it decays in 1 to 2 ps before a slower growth of STE absorption discussed above sets in. The fast initial population of STEs was shown by spectral analysis to amount to only a few percent of the initial population of free carriers, consistent with earlier calculations on BaF_2 [2,41]. The fact that the initially created STEs decay much faster than the STEs formed more slowly (i.e., ∼4 ps) upon bimolecular electron-hole recombination is unusual. An explanation that is consistent with many other parts of our basic conclusion is that the

initially created excitons are bathed in a population of hot free electrons for several picoseconds. Impact ionization by the hot free electrons constitutes a decay mechanism for the initially produced excitons, but not for the more slowly formed excitons in thermal equilibrium with the lattice. The decay of the slower STE population was shown to be affected on a 167-ps time scale even by very low Tl concentration of 0.0014 molar %. The STE decay time descended to 1–2 ps decay when the Tl concentration was raised about 30 times to 0.042 mole %.

The picosecond absorption measurements offer insight on a long-debated question of the relative importance of self-trapped exciton diffusion versus sequential capture of holes and electrons as the agents of energy transport from the halide scintillator host to the activator ion. In undoped CsI, the STE can be identified by its distinctive bound electron transitions at 0.5 and 0.7 eV. Adding Tl^+ at typically used concentration of about 0.01% was shown to destroy the infrared signature of STEs in about 2 ps. Does that STE destruction signify migration of the STE to Tl^+, or scavenging of the STE electron to create Tl^0? The STE hopping rate at room temperature in CsI is given by Kerisit *et al.* [55] as $1.3 \times 10^{10}\,s^{-1}$, generalizing from new theoretical findings that the activation barriers for STH and STE motion in NaI are about the same [49]. The STE hopping time of 80 ps corresponding to the above room-temperature rate is significantly slower than the observed time for scavenging or destruction of the STEs in CsI with 0.04 and 0.3 wt % Tl (estimated 0.006 and 0.04 mole % respectively). This suggests to us that electron tunneling to the nearest Tl^+ ion is the likely mechanism terminating the STE absorption signature when Tl is present at the indicated concentrations. To relate this to scintillation measurements, we note that Hamada *et al.* measured the rise and decay times of CsI:Tl luminescence for direct photoexcitation of the Tl ions and for high-energy excitation of the CsI host by 662-keV gamma rays [56]. The relatively slow ∼100 ns rising edge of the scintillation pulse at room temperature was attributed by Hamada *et al.* to STH diffusion [56]. In view of the above-mentioned recent theoretical finding that activation barriers for hopping of the STE and STH are about the same in NaI [49], the ∼100-ns rising component of scintillation might also be considered as due to STE migration. However, the picosecond absorption data reported here seem to rule out any significant population of STEs during the slow rise and extended decay of the scintillation pulse in CsI:Tl at working concentrations near 0.1% Tl. Even if STEs are formed much later by recombination of released electrons and self-trapped holes, the absorption data indicate that they would be electronically unstable in a lattice containing Tl^+, as concluded from Fig. 5. Sequential capture of holes and electrons on Tl^+ followed by migration of mainly electrons (Tl^0) on the Tl^+ sublattice until recombination creates Tl^{+*}, seems the transport route compatible with the picosecond absorption data in CsI:Tl and NaI:Tl. SrI_2:Eu still needs better identification of STE features to make a similar judgment.

Speculating that the 1-eV absorption in SrI_2 may be due to the STE and free carriers, Fig. 11 showed that doping with 3% Eu drives the decay to the remarkably short time scale of 800 fs, including the convoluted 500-fs laser pulse, implies a physical time for transfer from STE or free carriers to capture on 3% Eu^{2+} of about 400 fs. Such a fast excitation transfer from host to activator is consistent with the very high light yield of SrI_2:Eu, considerably higher than CsI:Tl or NaI:Tl.

ACKNOWLEDGMENTS

This work was supported by the Office of Nonproliferation Research and Development (NA-22) of the US Department of Energy under Contracts No. DE-AC02-05CH1123 and No. DE-NA0001012. We thank Q. Li (Wake Forest University), S. Kerisit (Pacific Northwest National Laboratory), and A. Vasilev (Moscow State University) for helpful discussions of electron thermalization and capture time, and N. Cherepy (Lawrence Livermore National Laboratory) for discussions of STE luminescence in SrI_2. We thank P. Bhattacharya, E. Tupitsyn, E. Rowe, V. M. Buliga (Fisk University) for preparation of SrI_2:Eu and S. Vasyukov (Institute for Scintillation Materials, Kharkov) for the preparation of NaI:Tl samples.

[1] J. Q. Grim, K. B. Ucer, A. Burger, P. Bhattacharya, E. Tupitsyn, E. Rowe, V. M. Buliga, L. Trefilova, A. Gektin, G. A. Bizarri, W. W. Moses, and R. T. Williams, Phys. Rev. B **87**, 125117 (2013).

[2] R. T. Williams, J. Q. Grim, Q. Li, K. B. Ucer, G. A. Bizarri, S. Kerisit, F. Gao, P. Bhattacharya, E. Tupitsyn, E. Rowe, V. M. Buliga, and A. Burger, in *SPIE Proceedings Vol. 8852, Hard X-Ray, Gamma-Ray, and Neutron Detector Physics XV* (SPIE, Bellingham, WA, 2013), pp. 88520J–1.

[3] Z. Wang, Y. Xie, B. D. Cannon, L. W. Campbell, F. Gao, and S. Kerisit, J. Appl. Phys. **110**, 064903 (2011).

[4] Z. Wang, Y. Xie, L. W. Campbell, F. Gao, and S. Kerisit, J. Appl. Phys. **112**, 014906 (2012).

[5] R. Kirkin, V. V. Mikhailin, and A. N. Vasil'ev, IEEE Trans. Nucl. Sci. **59**, 2057 (2012).

[6] A. Kozorezov, J. K. Wigmore, and A. Owens, J. Appl. Phys. **112**, 053709 (2012).

[7] Q. Li, J. Q. Grim, N. A. W. Holzwarth, and R. T. Williams, presented at the International Conference on Inorganic Scintillators and their Applications, SCINT, 2013 (unpublished).

[8] S. Kerisit (private communication).

[9] Q. Li, J. Q. Grim, K. B. Ucer, A. Burger, G. A. Bizarri, W. W. Moses, and R. T. Williams, Phys. Status Solidi RRL **6**, 346 (2012).

[10] J. Q. Grim, Q. Li, K. B. Ucer, A. Burger, G. A. Bizarri, W. W. Moses, and R. T. Williams, Phys. Status Solidi A **209**, 2421 (2012).

[11] M. S. Alekhin, J. T. M. de Haas, I. V. Khodyuk, K. W. Krämer, P. R. Menge, V. Ouspenski, and P. Dorenbos, Appl. Phys. Lett. **102**, 161915 (2013).

[12] R. T. Williams and M. N. Kabler, Phys. Rev. B **9**, 1897 (1974).

[13] R. T. Williams, J. N. Bradford, and W. L. Faust, Phys. Rev. B **18**, 7038 (1978).

[14] P. Martin, S. Guizard, P. Daguzan, G. Petite, P. D'Oliveira, P. Meynadier, and M. Perdrix, Phys. Rev. B **55**, 5799 (1997).

[15] T. Sugiyama, H. Fujiwara, T. Suzuki, and K. Tanimura, Phys. Rev. B **54**, 15109 (1996).

[16] T. Tokizaki, T. Makimura, H. Akiyama, A. Nakamura, K. Tanimura, and N. Itoh, Phys. Rev. Lett. **67**, 2701 (1991).

[17] R. T. Williams, M. N. Kabler, W. Hayes, and J. P. Stott, Phys. Rev. B **14**, 725 (1976).

[18] E. D. Thoma, H. M. Yochum, M. J. Binkley, M. Leblans, and R. T. Williams, in *Proceedings of the 13th International Conference on Defects in Insulating Materials, ICDIM 96* (Trans Tech Publications, Switzerland, 1997), pp. 565–568.

[19] H. Fujiwara, T. Suzuki, and K. Tanimura, in *Proceedings of the 13th International Conference on Defects in Insulating Materials, ICDIM 96* (Trans Tech Publications, Switzerland, 1997), pp. 561–564.

[20] R. T. Williams, K. B. Ucer, J. Q. Grim, K. C. Lipke, L. M. Trefilova, and W. W. Moses, IEEE Trans. Nucl. Sci. **57**, 1187 (2010).

[21] A. Alkauskas, C. E. Dreyer, J. L. Lyons, Q. Yan, and C. G. Van de Walle, APS March Meeting, Denver, CO (APS, Melville, NY, 2014).

[22] V. Pankratov, A. I. Popov, L. Shirmane, A. Kotlov, G. A. Bizarri, A. Burger, P. Bhattacharya, E. Tupitsyn, E. Rowe, V. M. Buliga, and R. T. Williams, Radiat. Meas. **56**, 13 (2013).

[23] V. A. Pustovarov, I. N. Ogorodnikov, A. A. Goloshumova, L. I. Isaenko, and A. P. Yelisseyev, Opt. Mater. **34**, 926 (2012).

[24] O. Sidletskiy, in *Crystal Growth Technology: Semiconductors and Dielectrics*, edited by P. Capper and P. Rudolph (Wiley VCH, Weinheim, 2010), Chap. 16.

[25] N. Cherepy, L. Boatner, A. Burger, K. Shah, S. Payne, A. Janos, and A. Kuhn, LLNL Presentation No. LLNL-PRES-426327 (unpublished).

[26] H. Nishimura, M. Sakata, T. Tsujimoto, and M. Nakayama, Phys. Rev. B **51**, 2167 (1995).

[27] K. Edamatsu, M. Sumita, S. Hirota, and M. Hirai, Phys. Rev. B **47**, 6747 (1993).

[28] R. M. Van Ginhoven, J. E. Jaffe, S. Kerisit, and K. M. Rosso, IEEE Trans. Nucl. Sci. **57**, 2303 (2010).

[29] D. Fröhlich, B. Staginnus, and Y. Onodera, Phys. Status Solidi B **40**, 547 (1970).

[30] K. Teegarden and G. Baldini, Phys. Rev. **155**, 896 (1967).

[31] H. F. Ivey, Phys. Rev. **72**, 341 (1947).

[32] F. Stöckmann, Naturwissenschaften **39**, 226 (1952).

[33] M. Itoh, K. Tanimura, and N. Itoh, J. Phys. Soc. Jpn. **62**, 2904 (1993).

[34] V. A. Kravchenko, V. M. Lisitsyn, and V. Y. Yakovlev, Fizika Tverdogo Tela **28**, 3473 (1986).

[35] W. B. Fowler, *Physics of Color Centers* (Academic, New York, 1968), Chap. 2 and Appendix B.

[36] Q. Li, R. T. Williams, and D. Aberg, Phys. Status Solidi B **250**, 233 (2013).

[37] R. T. Williams, C. L. Marquardt, J. W. Williams, and M. N. Kabler, Phys. Rev. B **15**, 5003 (1977).

[38] K. B. Ucer, R. A. Wall, K. C. Lipke, and R. T. Williams, Phys. Status Solidi B **245**, 2680 (2008).

[39] J. I. Pankove, *Optical Processes in Semiconductors* (Dover, New York, 1971), pp. 75–76.

[40] D. A. Clugston and P. A. Basore, Prog. Photovoltaics **5**, 229 (1997).

[41] A. Vasil'ev and A. Gektin, in *Proceedings of the 8th International Conference on Inorganic Scintillators and their Applications (SCINT2005)*, edited by B. Grinyov and A. Gektin (National Academy of Sciences of Ukraine, Kharkov, 2006), pp. 1–6.

[42] E. S. Gafiatulina, S. A. Chernov, and V. Y. Yakovlev, Phys. Solid State **40**, 586 (1998).

[43] T. Sidler, J. P. Pellaux, N. A, and M. A. Aegerter, Solid State Commun. **13**, 479 (1973).

[44] V. Yakovlev, L. Trefilova, and A. Meleshko, J. Lumin. **129**, 790 (2009).

[45] S. A. Chernov, L. Trinkler, and A. I. Popov, Radiat. Eff. Defects Solids **143**, 345 (1998).

[46] J. M. Spaeth, W. Meise, and K. S. Song, J. Phys.: Condens. Matter **6**, 3999 (1994).

[47] V. Yakovlev, L. Trefilova, A. Meleshko, V. Alekseev, and N. Kosinov, presented at the International Conference on Advanced Scintillation Materials, Kharkov, Ukraine (unpublished).

[48] K. S. Song and R. T. Williams, *Self-Trapped Excitons*, Series in Solid State Sciences, Vol. 105 (Springer, Berlin, 1993).

[49] P. Erhart, A. Schleife, B. Sadigh, and D. Åberg, Phys. Rev. B **89**, 075132 (2014).

[50] B. W. Sturm, N. J. Cherepy, O. B. Drury, P. A. Thelin, S. E. Fisher, S. P. O'Neal, S. A. Payne, A. Burger, L. A. Boatner, J. O. Ramey, K. S. Shah, and R. Hawrami, in *Nuclear Science Symposium and Medical Imaging Conference (NSS/MIC)* (IEEE, Washington, DC, 2011), pp. 7–11.

[51] N. J. Cherepy, S. A. Payne, B. W. Sturm, O. B. Drury, S. P. O'Neal, P. A. Thelin, K. S. Shah, R. Hawrami, M. Momayezi, B. Hurst, A. Burger, B. Wiggins, P. Bhattacharya, L. A. Boatner, and J. O. Ramey, IEEE Trans. Nucl. Sci. **60**, 955 (2013).

[52] G. A. Bizarri, A. Burger, and R. T. Williams (unpublished).

[53] E. D. Thoma, H. M. Yochum, and R. T. Williams, Phys. Rev. B **56**, 8001 (1997).

[54] A. Belsky, K. Ivanovskikh, A. Vasil'ev, M.-F. Joubert, and C. Dujardin, J. Phys. Chem. Lett. **4**, 3534 (2013).

[55] Z. Wang, R. T. Williams, J. Q. Grim, F. Gao, and S. Kerisit, Phys. Status Solidi B **250**, 1532 (2013).

[56] M. M. Hamada, F. E. Costa, M. C. C. Pereira, and S. Kubota, IEEE Trans. Nucl. Sci. **48**, 1148 (2001).